

Research Article

Research on nonlinear corrosion law of epoxy coating on steel bridges based on image processing

Yi Zhang^a, Tian Su^{*,b}

Department of Engineering and Management, International College, Krirk University, Bangkok, Thailand

Article Info

Abstract

Article history:

Received 25 Mar 2024
Accepted 05 June 2024

Keywords:

Image processing;
Steel bridge coating;
Non linearity;
Corrosion law

This paper adopted the accelerated corrosion test method to study the corrosion law of epoxy coatings on steel bridges. An image processing algorithm based on MATLAB was used to perform grayscale conversion, normalized histogram drawing, and binary image processing on the surface morphology images of coated specimens. Four coated specimens were prepared and placed in the cyclic accelerated corrosion environment. The coated specimens were subjected to the accelerated corrosion test for 90 days, observed changes in coating thickness and corrosion area rate and analyzing the corrosion laws of epoxy coatings in different corrosion environments. Using image processing technology to process images of coating corrosion and analyze the corrosion mechanism of coatings. The research results indicate that the corrosion rate of epoxy coatings exhibits a non-linear corrosion law of slow corrosion in the early stage and accelerated corrosion in the middle and later stages. The corrosion rate of epoxy coatings in saltwater corrosive environments is faster than in freshwater corrosive environments. Based on the corrosion laws and mechanisms of coatings, a nonlinear corrosion function model for epoxy coatings on steel bridges under different accelerated corrosion environment was established, which has a high correlation with experimental data.

© 2024 MIM Research Group. All rights reserved.

1. Introduction

Corrosion is a phenomenon in which metals undergo chemical or electrochemical reactions with the surrounding environment, causing significant economic losses and social harm to various industries [1-2]. Steel exposed to the atmosphere is prone to chemical reactions caused by the combined effects of environmental factors such as oxygen and rainwater (acid rain), leading to the formation of rust [3-5]. If severe corrosion occurs in key parts of the steel bridge, it may pose a threat to the structural bearing capacity of the steel bridge. To prevent the corrosion of steel by air and water, anti-corrosion coating technology has emerged as the most commonly used means to slow down the corrosion rate of steel bridges. The principle of most coatings for corrosion prevention is mainly physical corrosion prevention, which is achieved by coating the steel surface to avoid direct contact between air and water on the steel [6-8]. At present, the most widely used anti-corrosion method for steel bridges is to apply coatings on the surface of the steel bridge. However, during the service of steel bridges, the coating will also undergo corrosion and aging due to environmental factors such as oxygen, rainwater, and ultraviolet radiation. As the corrosion intensifies, the protective effect of the coating on the steel bridge becomes increasingly worse. Therefore, in order to effectively control the corrosion of steel bridges and extend their service life, the corrosion law of steel bridge coatings has become a topic worthy of in-depth research.

*Corresponding author: sutiancivil@foxmail.com

^a orcid.org/0009-0001-6911-8125; ^b orcid.org/0000-0002-1851-2288

DOI: <http://dx.doi.org/10.17515/resm2024.219ma0325rs>

Res. Eng. Struct. Mat. Vol. x Iss. x (xxxx) xx-xx

During the visual inspection process by coating inspectors, due to the diverse types and complex presentation of coating defects, it is difficult for inspectors to identify the specific types of defects. Moreover, visual errors can also make it difficult to detect subtle defects, such as pitting, micro bubbles, and filamentous cracks, when observed with the naked eye. When measuring defects, traditional measuring instruments are used, and ensuring the measurement accuracy required for corrosion inspection in an on-site environment is difficult. Moreover, there are no effective measuring tools for irregular coating defects, such as those for measuring the area of rust and peeling. With the development of image acquisition technology and image processing technology, the identification and measurement of corrosion defects encountered in the inspection process of coating defects mentioned above will be effectively improved. Image processing technology is a technique that uses image processing algorithms to process and optimize images captured by digital cameras and other tools to achieve the desired results [9]. The main steps of image processing include contrast enhancement, filtering, threshold segmentation, morphological processing, feature extraction and classification [10].

In the field of corrosion, the form and characteristics of corrosion damage can be represented by corrosion images to evaluate the type of corrosion and analyze the degree of corrosion. The corrosion images become an important basis for studying corrosion laws. By establishing appropriate segmentation criteria and recognition models, quantitative description of corrosion areas can be obtained. Corrosion detection problems can be transformed into computer vision problems [11-13]. The traditional image processing method is to use wavelet transform to extract energy and entropy values from each sub image of the corrosion image, and use them to detect the corrosion area in the image [14-15]. Scholars have used the color difference between corroded and non-corroded areas to segment images [16]. Some scholars also believe that as corrosion intensifies, the roughness of the metal surface also changes, which is reflected in the corrosion image [17]. The gray scale values of pixels at the corrosion edge are different from those at other locations, and this distinguishes between corroded and non-corroded areas [18-19]. Furthermore, several scholars have proposed using Non-Destructive Evaluation (NDE) to analyze texture changes on corroded surfaces, combined with Self Organizing Feature Mapping (SOFM) networks for corrosion damage classification, or training Support Vector Machines (SVM) for corrosion classification and detection, based on the color characteristics of the corroded area [20-22].

In the study of coating corrosion laws, the commonly used method is to compare and evaluate the physical, chemical, and electrochemical properties of coatings as they decay with exposure time, in order to establish a model for the variation of coating corrosion laws. Many scholars have conducted research on the corrosion laws of coatings. Kim et al. [23] conducted accelerated exposure tests on five commonly used coating systems for Japanese steel bridges and discussed the corrosion degradation caused by initial coating defects. Hirohata et al. [24] developed an accelerated exposure experimental system to simulate seawater environment. The acceleration coefficient of this experimental system is based on the study of the actual corrosion depth of structural steel components exposed to seawater environment for more than 19 years. Kallias et al. [25] reviewed the mechanisms that lead to coating degradation, with a focus on the main types of coatings. Based on the classification of corrosive environments and response function models, research was conducted to quantify the impact of corrosion, and an atmospheric corrosion model was proposed. Kendig et al. [8] studied the anti-corrosion performance of organic coatings using electrochemical impedance method and established a life prediction model for organic coatings. Lee et al. [26] studied the life of coatings through on-site exposure tests and artificial accelerated aging tests, and established aging models for three coating systems: chlorinated rubber, polyurethane, and inorganic zinc rich. Through regression

analysis, the life prediction formulas for the three coating systems were obtained, and the life of the three coating systems were found to be 20.8 years, 26.6 years, and 17.8 years, respectively. Fredj et al. [27-29] used electrochemical impedance spectroscopy to study the protective performance of organic coatings under the coupling effect of load and corrosive environment. By comparing and analyzing the effects of different loads and stress symbols on the protective performance of organic coatings, the results showed that tensile stress accelerated the degradation of coatings, while compressive stress slowed down the loss of coating performance. The S6-cycle corrosion test was carried out on structural steels for 30, 60, 90, 120 and 150 days and metal coating films for 100, 200 and 300 days [30]. The purpose of this study was to determine correlation between an accelerated cyclic corrosion test (S6-cycle test) specified in Japanese Industrial Standards K5621 and field exposure tests. Merachtsaki et al. [31] studied the corrosion behavior of steel coated with epoxy-(organo) clay nanocomposite films by using salt spray exposures, optical and scanning electron microscopy examination, open circuit potential, and electrochemical impedance measurements. Rachid [32] reviewed the chemical corrosion mechanism and calculation method of the corrosion behavior of epoxy anti-corrosion coatings in 3.5% NaCl solution.

Based on image processing technology, this paper adopted the accelerated corrosion test method to study the corrosion law of epoxy coatings on steel bridges. Four coated specimens were prepared and placed in a cyclic accelerated corrosion environment. The coated specimens were subjected to a 90-day accelerated corrosion test to observe changes in coating thickness and corrosion area rate, and to analyze the corrosion laws of epoxy coatings in different corrosion environments. Image processing technology was used to process images of coating corrosion and analyze the corrosion mechanism of coatings. The research results indicate that the corrosion rate of epoxy coatings exhibits a nonlinear corrosion pattern of slow corrosion in the early stage and accelerated corrosion in the middle and later stages. The corrosion rate of coatings in saline corrosive environments is faster than in freshwater corrosive environments. Based on the corrosion laws and mechanisms of coatings, a nonlinear corrosion function model for epoxy coatings on steel bridges under different accelerated corrosion environments was established, which has a high correlation with experimental data.

2. Materials and Experimental Procedure

2.1. Materials

The coating systems widely used on steel bridges mainly include epoxy coating systems, acrylic polyurethane coating systems, and fluorocarbon coating systems. The research object of this paper is the epoxy coating system. Details of epoxy coating in this paper are as shown in table 1. Four epoxy coated specimens were prepared with specimen numbers HY01, HY02, HY03, and HY04, respectively. Q235 low-carbon steel with a size of 140mm×70mm×4.5mm was selected as the sample steel plate, which has good thermal conductivity and corrosion resistance.

Table 1. Details of epoxy coating in this paper

Parameters	Epoxy Coating
Substrate	Mild steel
preparation grades	Sa 2.5
primer	inorganic zinc rich (50 μm)
intermediate coat	epoxy cloud iron (100μm)
top coat	epoxy topcoat (50μm)
Color	gray
Dry film thickness	(200±40)μm

Prior to abrasion, the Q235 cold-rolled mild steel panels were cleaned with a metal cleaner, used to remove excess oil from the surface of the steel panels, and then dried at room temperature [33]. The surfaces of both the sample and the base plate were pretreated before painting, a polishing machine was used to polish them to the Sa2.5 level, and then the sample was prepared by painting [34]. After each coating, the samples were cured at room temperature for 24 hours, after which the second layer of paint was applied at room temperature. After each coating was brushed and cured, a coating thickness gauge was used for testing to achieve the required coating thickness range. The coating thickness standard was inorganic zinc-rich (50 μm) + epoxy cloud iron (100 μm) + epoxy topcoat (50 μm), with a spraying thickness not exceeding 20% of the standard thickness. The coated specimens are as shown in Fig. 1.

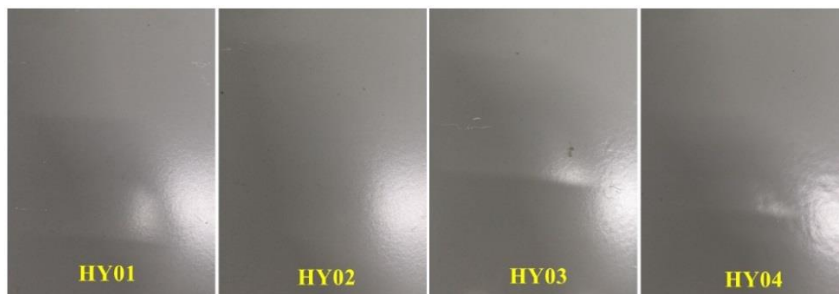


Fig. 1. Preparation of coated specimens

2.2. Cyclic Accelerated Corrosion Test

To simulate the service environment of steel bridges more realistically, this paper designs a cyclic accelerated corrosion test involving a water environment immersion test and an accelerated aging test. The cycling program for the accelerated corrosion test was set as follows: 144 h accelerated aging test+72 h water environment immersion test.

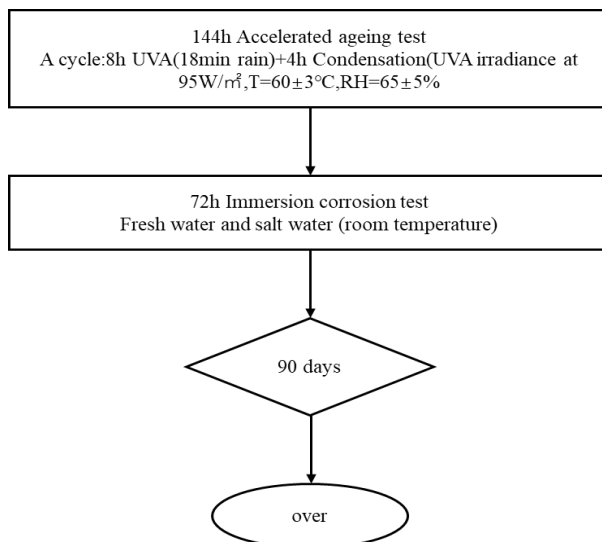


Fig. 2. Cyclic Accelerated Corrosion Test Procedure

The cyclic accelerated corrosion test procedure is shown in Fig. 2. To complete the water environment corrosion test, a water environment corrosion test chamber was constructed, and a total of two water environment corrosion test chambers were prepared: a freshwater environment corrosion test chamber (the water source for the devices inside the chamber was tap water) and a saline environment corrosion test chamber (the water source for the devices inside the chamber was 3.5% sodium chloride solution). The accelerated aging test is completed through an accelerated aging environment test chamber, which can control the intensity, humidity, and temperature of ultraviolet radiation. The cycle program of the accelerated aging test included 8 hours of ultraviolet radiation (including 18 minutes of rain) +4 hours of condensation, where the ultraviolet intensity was 95 W/m^2 , the temperature was $60 \pm 3^\circ\text{C}$, and the relative humidity was $65 \pm 5\%$. The duration of the experimental plan in this article was 90 days, and the coating thickness and corrosion area rate of each coated specimen were measured every 10 days. After measurement, the initial coating thickness of all 4 coated specimens was $200 \mu\text{m}$, and the initial corrosion area rate was 0%. The test environment for epoxy coated specimens is shown in Table 2.

Table 2. Test environment for coating specimens

Coating test piece number	Test environment
HY01	Freshwater + Accelerated aging test
HY02	
HY03	Saltwater + Accelerated aging test
HY04	

2.3. Coating Performance Testing Methods

A CT-220 coating thickness gauge was used to measure the thickness changes of the coating during the corrosion process. Before measurement, the instrument was calibrated on a standard metal block to confirm that the measurement accuracy met the requirements. Each coating specimen was measured at 5 points, and the arithmetic mean of the 5 measurement values was taken as the coating thickness of the specimen; A camera was used to capture photos of the coating surface, image processing technology was used to process the surface appearance image of the corroded coating, and the change in the rust area rate of the coating was calculated.

3. Test Results

3.1. Coating Thickness

The transmission of corrosive media such as water and oxygen in coatings conforms to Fick's diffusion law, and when a coating is used to protect the surface of a steel plate, a coating film is formed on the surface of the steel plate. This coating film can block the contact between corrosive media and the steel substrate. Based on this theory, many scientific and technological workers believe that increasing the coating thickness can increase the protective effect of the coating on the steel, thereby extending the service life of the coating. Therefore, coating thickness is one of the important indicators reflecting the corrosion process of coatings.

Fig. 3 and Fig. 4 respectively show the variation of coating thickness and coating thickness loss rate with test time for epoxy coated specimens placed in different accelerated corrosion environments. From the graph, it can be seen that the coating thickness of the freshwater environment specimens (HY01 and HY02) increased from the initial thickness of $200 \mu\text{m}$ during a 90 day accelerated corrosion test time dropped to $173 \mu\text{m} \sim 174 \mu\text{m}$. The loss value of coating thickness is $26 \mu\text{m} \sim 27 \mu\text{m}$. The loss rate of coating thickness is

13.0%~13.5%. During a 90 day accelerated corrosion test, the coating thickness of the saltwater environment specimens (HY03 and HY04) increased from the initial thickness of 200 μm dropped to 170 μm ~171 μm . The loss value of coating thickness is 29 μm ~30 μm . The loss rate of coating thickness is 14.5%~15.0%. The phenomenon of coating thickness loss is due to the combined effect of factors such as ultraviolet radiation, water, and oxygen on the coating in an accelerated corrosion environment, especially the significant impact of ultraviolet radiation on the decrease of coating thickness. Ultraviolet radiation can decompose the ion bonds between the high polymers of the coating, leading to aging and degradation of the coating. The surface of the coating gradually becomes powdery, and the residue of coating decomposition gradually separates from the coating under the washing of water. This pulverization and erosion effect leads to a gradual decrease in coating thickness. The experimental results show that regardless of whether it is in a freshwater or saline environment, the coating thickness gradually decreases with the extension of the test time, and shows a slow decrease in coating thickness in the early stage of corrosion, and a faster decrease in coating thickness in the middle and later stages of corrosion. This indirectly indicates that the corrosion rate of the coating follows a non-linear corrosion pattern of slow corrosion in the early stage and accelerated corrosion in the middle and later stages.

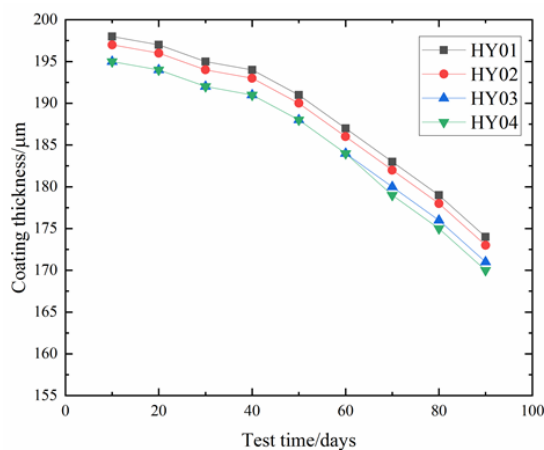


Fig. 3. The variation law of coating thickness with test time

According to the change in coating thickness data, the coating thickness of specimen HY01 decreased by 26 μm , and the coating thickness of specimen HY03 decreased by 29 μm . From the perspective of coating thickness loss, the coating thickness loss of specimens in saline environment (HY03 and HY04) is greater than that of specimens in freshwater environment (HY01 and HY02). This indicated that the corrosion rate of epoxy coatings on steel bridges in saline accelerated corrosion environment is faster than that in freshwater accelerated corrosion environment. For epoxy coatings, in saline corrosive environments, they not only face corrosion from UV rays, water, oxygen, etc., but also from chloride ions. Chloride ions can accelerate the chemical reaction that occurs during coating corrosion, leading to an accelerated rate of molecular decomposition of the coating. The experimental results indicate that chloride ions in saline environments can accelerate the corrosion rate of epoxy coatings.

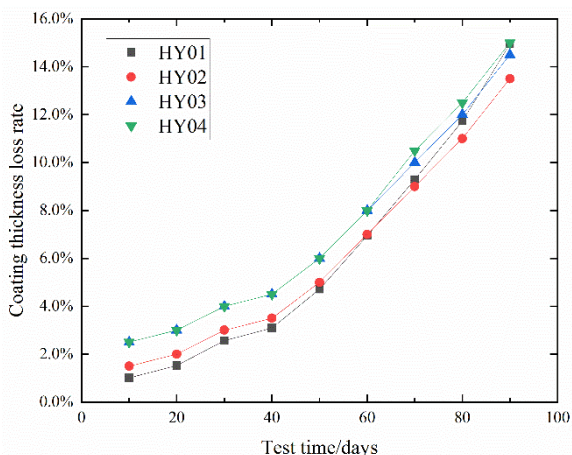


Fig. 4. The variation law of coating thickness loss rate with test time

3.2. Corrosion Area Rate

The corrosion area of the coating is the most effective indicator for characterizing the corrosion process and health status of the coating. When the corrosion area rate reaches a specific value, it can be considered that the coating has failed. This article takes the corrosion area rate of coatings as one of the research indicators to analyze the corrosion laws of coatings.

Fig. 5 shows the variation in the corrosion area rate of epoxy coated steel bridge specimens in different accelerated corrosion environments over time. The graph shows that during the 90-day accelerated corrosion test period, the corrosion area rate of the freshwater environment specimens increased from 0% to 1.90%. In the range of 0-40 days, the corrosion area rate of the coating remained at 0%. In the range of 40-90 days, the corrosion area rate of the coating gradually increased, and the slope of the increase became increasingly larger. During the 90-day accelerated corrosion test period, the corrosion area rate of the saline environment specimens increased from 0% to 2.40%. In the range of 0-20 days, the corrosion area rate of the coating remained at 0%. In the range of 20-90 days, the corrosion area rate of the coating gradually increased, and the slope of the increase became increasingly larger. The experimental results show that with increasing test time, the corrosion area rate gradually increases, the corrosion area rate slowly increases in the early stage of corrosion, and the corrosion area rate rapidly increases in the middle and late stages of corrosion, indicating that the coating corrosion process follows a nonlinear corrosion law. The increase in corrosion area is due to the combined effect of factors such as UV radiation, water, and oxygen on the coating in an accelerated corrosion environment, leading to electrochemical reactions of the coating. The coating gradually undergoes corrosion degradation, losing its protective effect on the steel bridge structure. The nonlinear corrosion law may be because in the early stage of corrosion, the loss of coating thickness is relatively small, and the insulating effect of the coating against external erosion factors is still strong. Oxygen, water, chloride ions, etc. need a long time to enter the coating substrate; In the middle and later stages of corrosion, as the thickness of the coating decreases and the porosity of the coating gradually increases, corrosion factors are more likely to enter the coating substrate and undergo chemical reactions, accelerating the electrochemical reaction process of coating corrosion. The accumulation rate of corrosion products is greatly accelerated, characterized by an accelerated increase in the corrosion area rate of the coating.

From the perspective of the change in corrosion area rate, the corrosion area rate of specimens in saline environment (HY03 and HY04) increased faster than that in freshwater environment (HY01 and HY02), indicating that the corrosion rate of the epoxy coating on steel bridges in saline accelerated corrosion environment is faster than that in freshwater accelerated corrosion environment. By comparing the composition factors of saline corrosion environment and freshwater corrosion environment, it can be concluded that chloride ions are the main factor affecting coating corrosion in saline corrosion environment. For epoxy coatings, chloride ions have a smaller radius and are more likely to penetrate the coating and enter the coating/metal interface. Prolonged exposure of chloride ions in aqueous solutions can accelerate corrosion reactions and easily penetrate the protective film on the metal surface, causing crevice corrosion and pore corrosion.

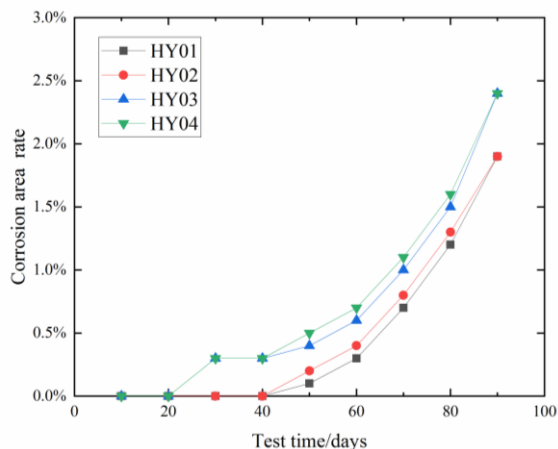


Fig. 5. The variation law of corrosion area rate with test time

3.3. Coating Corrosion Morphology Based on Image Processing

At present, the quality inspection of coating surfaces mainly relies on manual work. The manual corrosion detection of coating surfaces is limited by its subjectivity, making it difficult to objectively quantify the characteristics of corrosion. In recent years, image processing technology has gradually been applied in the field of coating corrosion. The form and characteristics of coating corrosion damage can be represented by corrosion images to evaluate the type of corrosion and analyze the degree of corrosion. This is important basis for studying corrosion laws.

To obtain clearer and easier to recognize images of the coating corrosion morphology, this paper adopts an image processing algorithm based on MATLAB to perform grayscale conversion, normalized histogram drawing, and binary image processing on the surface morphology images of coated specimens. Fig. 6 shows the corrosion morphology image of the coating after cyclic accelerated corrosion test. From the graph, it can be seen that the number of corrosion rust points in the saltwater environment coated specimens is significantly higher than that in the freshwater environment coated specimens, which is consistent with the variation law of the corrosion area rate of the coating. This indirectly confirms that chloride ions can accelerate the corrosion of the coating. Compared with the initial morphology of the coating, the color of the coating has undergone significant changes. This is mainly because the pigment molecules in the coating are excited to form free radicals after being exposed to ultraviolet radiation, leading to molecular breakage and chemical changes, resulting in a change in color. Fig. 7 shows a grayscale image of

coating corrosion morphology, which is generated by converting a three-dimensional RGB image into a two-dimensional grayscale image through image processing algorithms. Fig. 8 and Fig. 9 show the normalized histograms of coating corrosion morphology images, which can directly reflect the ratio of different grayscale levels. The horizontal axis represents the grayscale level of each pixel in the image, and the vertical axis represents the number or probability of pixels with different grayscale levels appearing in the image. Normalized histograms are of great significance in obtaining the optimal threshold for images.

Fig. 10 and Fig. 11 show binary images of coating corrosion morphology. The method of generating binary images is to obtain the assumed optimal threshold of the image based on the normalized histogram, calculate the center values of the foreground and background at this threshold. When the average value of the center values of the foreground and background is the same as the assumed optimal threshold, the iteration is terminated. This value is used as the threshold for binarization. From the graph, it can be seen that after the cyclic accelerated corrosion test for 90 days, the surface of the coated specimens showed varying degrees of corrosion. The corrosion area rate of the coated specimens in a saline environment was greater. Therefore, image processing algorithms based on MATLAB can clearly present the corrosion morphology and degree of coating corrosion.

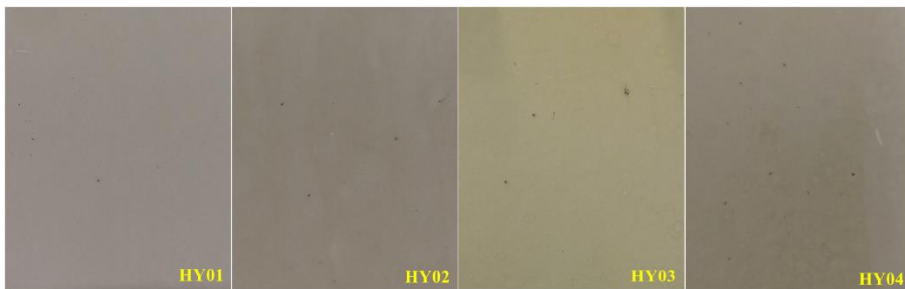


Fig. 6. Coating corrosion morphology at 90 days

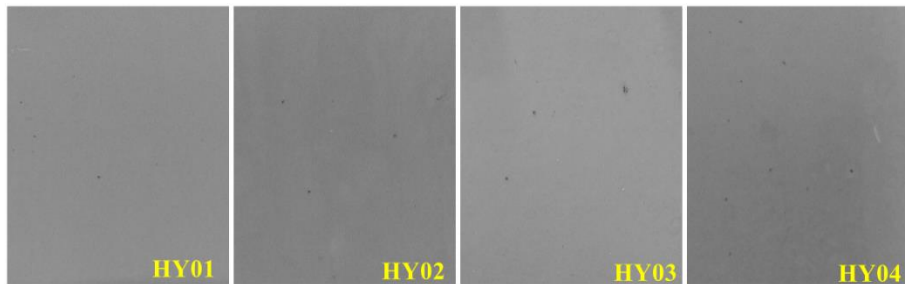


Fig. 7. Gray scale image of coating corrosion morphology at 90 days

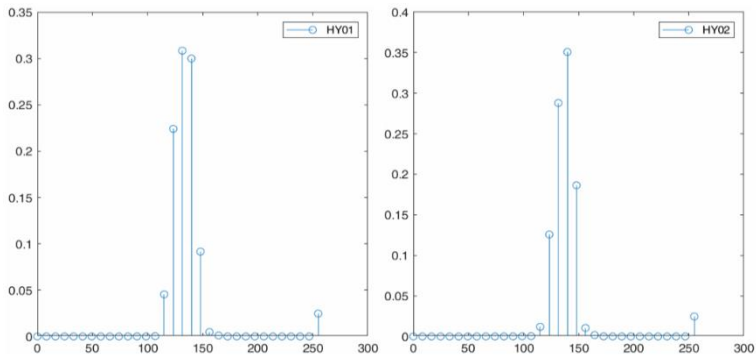


Fig. 8. Normalized histogram of coating corrosion images at 90 days (HY01 and HY02)

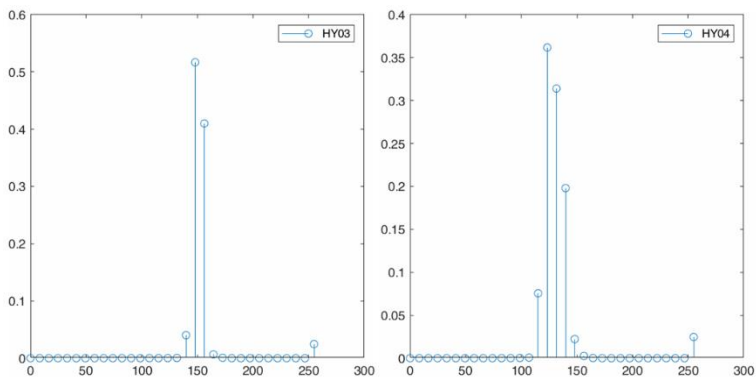


Fig. 9. Normalized histogram of coating corrosion images at 90 days (HY03 and HY04)

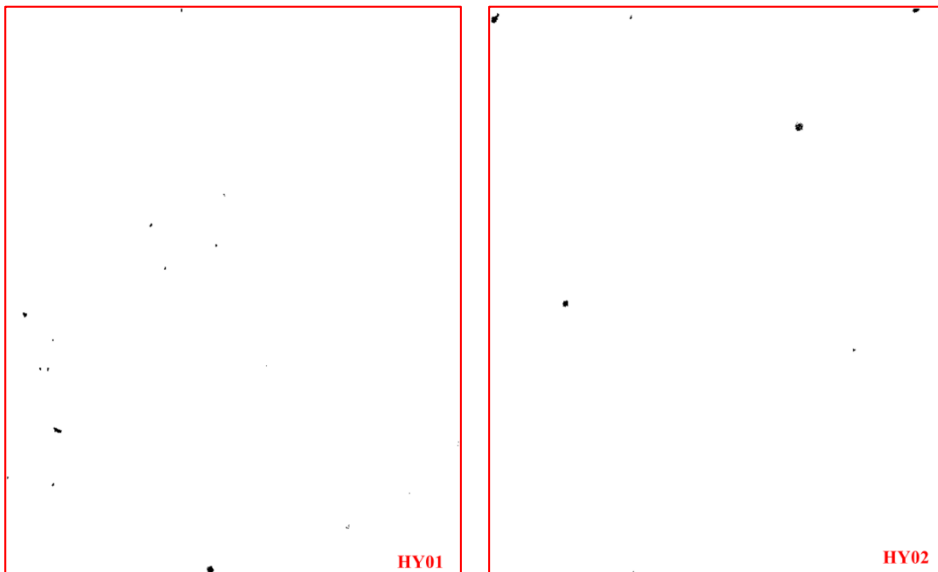


Fig. 10. Binary image of coating corrosion morphology (HY01 and HY02)

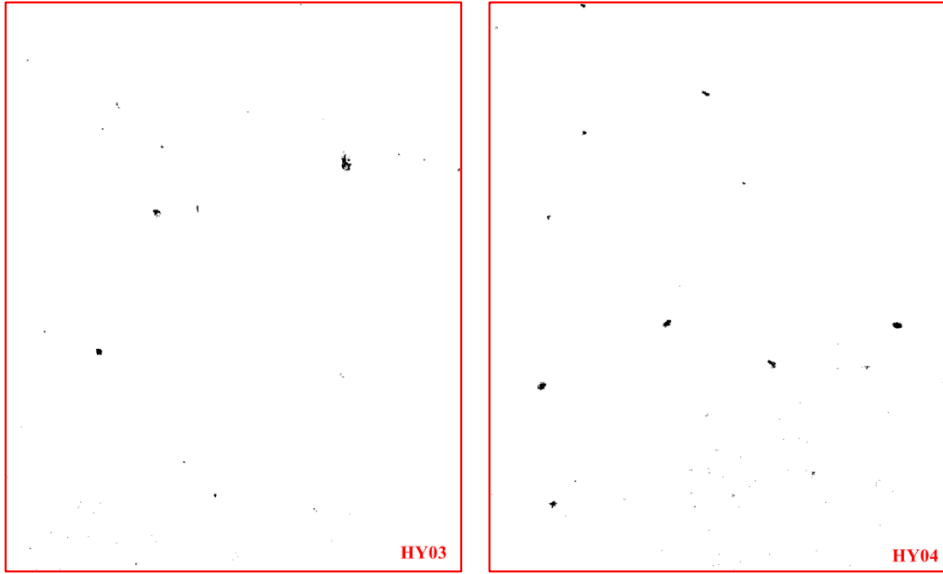


Fig. 11. Binary image of coating corrosion morphology (HY03 and HY04)

4. Discussion

4.1. Analysis of Corrosion Data

To reduce the error of experimental data, the average coating thickness loss rate of epoxy coated specimens was fitted and analyzed. Nonlinear corrosion function fitting was performed for two corrosion conditions, namely epoxy coating in freshwater environment and epoxy coating in saltwater environment, respectively. Fig. 12 and Fig. 13 respectively show the fitting curves of coating thickness loss rate under different corrosion environment. After fitting with Origin Pro2019 software, there is a high correlation between the coating thickness loss rate and the quadratic polynomial.

$$H = n + B_1 \times t + B_2 \times t^2 \quad (1)$$

Where, H represents the loss rate of coating thickness, t represents the corrosion time of the coating (in days). n , B_1 , and B_2 are constants (different corrosion environment correspond to different values, see Table 3 for parameter values).

Table 3. Parameter values under different corrosion environment

Corrosion Environment	n		B_1		B_2		R^2
	Value	Standard Error	Value	Standard Error	Value	Standard Error	Correlation
Freshwater	0.0047	0.0027	2.26E-4	1.42E-4	1.43E-5	1.52E-6	0.99
Saltwater	0.0090	0.0047	6.08E-4	2.42E-4	1.01E-5	2.59E-6	0.98

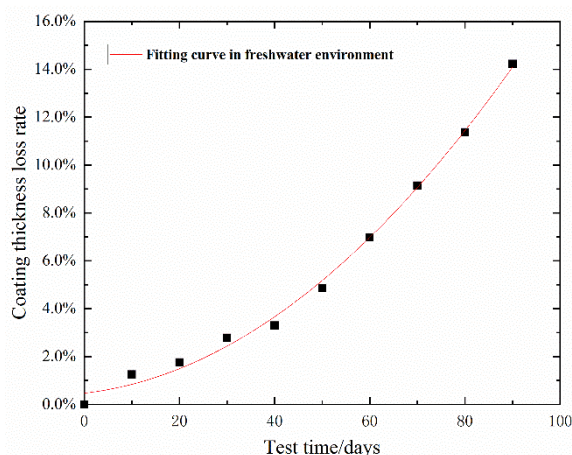


Fig. 12. Fitting curve of thickness loss rate of epoxy coating in freshwater environment

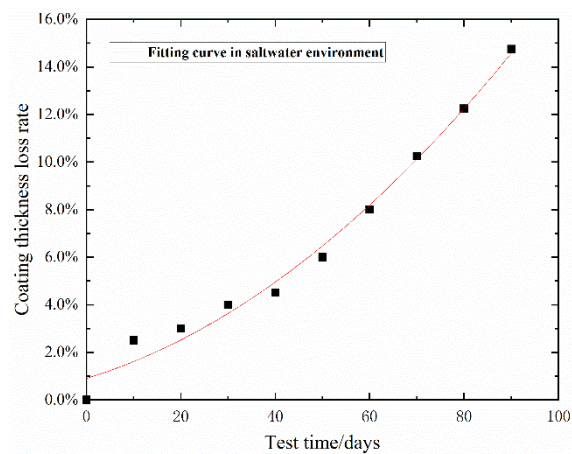


Fig. 13. Fitting curve of thickness loss rate of epoxy coating in saltwater environment

Due to the possibility of deviation in the corrosion area rate of individual coated specimens, this article takes the average corrosion area rate of specimens under the same conditions for data fitting to reduce model errors. Nonlinear corrosion function fitting is performed on epoxy coatings in freshwater and saline environment. Fig. 14 and Fig. 15 respectively show the fitting curves of corrosion area rate under different corrosion environment. After fitting with Origin Pro2019 software, there is a high correlation between the corrosion area rate of the coating and the following functional models.

$$S = a \times b^t \tag{2}$$

Where, S: corrosion area rate, t: corrosion time (days), a and b: constant (different corrosion environment correspond to different values, see Table 4 for parameter values).

Table 4. Parameter values under different corrosion environment

corrosion environment	a		b		R^2
	value	standard error	value	standard error	correlation
Freshwater	2.98E-10	2.22E-10	4.00	0.1677	0.99
Saltwater	3.76E-08	3.81E-08	2.96	0.2302	0.98

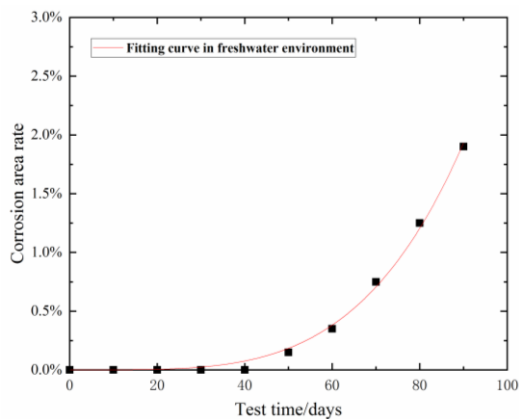


Fig. 14. Fitting curve of corrosion area rate of epoxy coating in freshwater environment

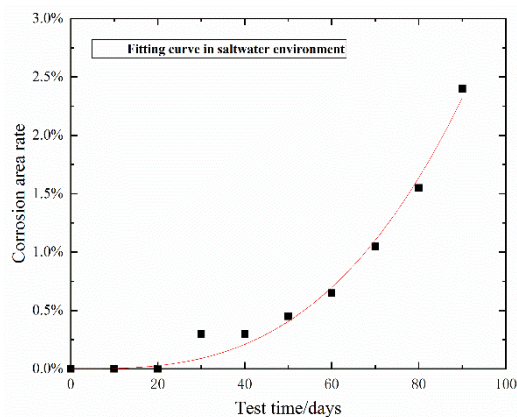


Fig. 15. Fitting curve of corrosion area rate of epoxy coating in saltwater environment

4.2. Analysis of Corrosion Mechanism of Epoxy Coatings

The experimental results of this paper indicate that the corrosion rate of epoxy coatings exhibits a non-linear corrosion pattern of slow corrosion in the early stage and accelerated corrosion in the middle and later stages. The schematic diagram of the coating corrosion process is shown in Fig. 16. Based on the experimental phenomena and results in this article, the corrosion mechanism of epoxy coatings on steel bridges is analyzed as follows the epoxy coating is a multi-layer structure, and in the early stage of corrosion, the pores of the coating are very dense, making it difficult for corrosive substances such as air, water, and chloride ions to pass through the coating and reach the coating/metal substrate

interface. With the passage of time, the effects of ultraviolet radiation, temperature changes, humidity changes, and other factors cause the polymer structure of the coating to continuously age and degrade. The pores of the coating become less dense, and substances such as oxygen and water can partially enter the interior of the coating through the pores and undergo chemical reactions. Therefore, in the early stage of coating corrosion, it is generally manifested as coating powdering, color difference, loss of glossiness, etc. There will be no rust spots, coating peeling in the early stage of coating corrosion. With the development of corrosion process, the corrosion rate continues to accelerate, and the decomposition rate of coating material structure is also accelerating.

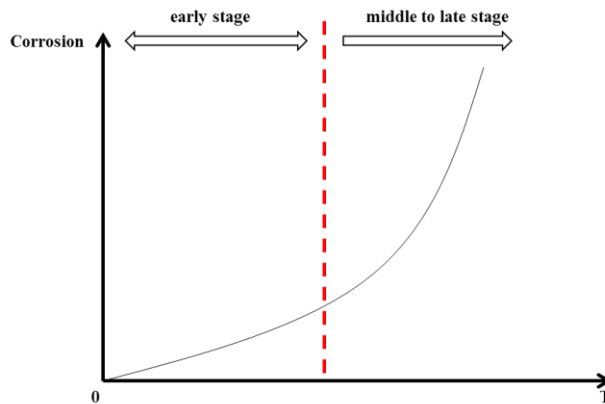


Fig. 16. The schematic diagram of the coating corrosion process

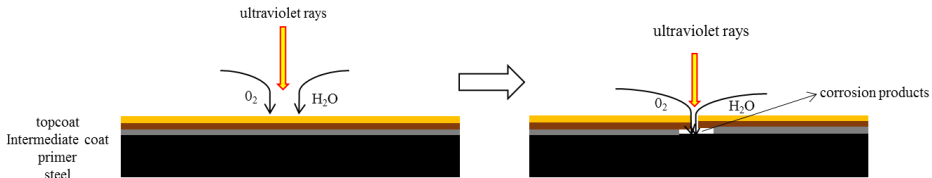


Fig. 17. The corrosion mechanism of epoxy coating under freshwater environment

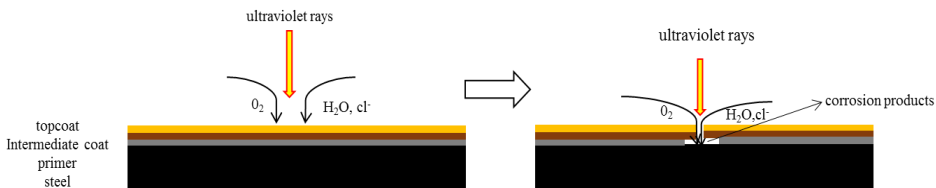


Fig. 18. The corrosion mechanism of epoxy coating under freshwater environment

The chemical reaction rate at the coating/metal matrix interface continues to accelerate. The generated chemical reaction products continue to accumulate and increase. The coating will expand, forming obvious corrosion problems such as rust spots, bubbles, and even coating peeling. Therefore, when the corrosion process reaches the middle and later stages, the rate of coating corrosion will greatly accelerate, and the products of coating corrosion degradation will continue to increase, ultimately manifested as the continuous expansion of the corrosion area rate. When the corrosion area rate increases to a specific

value, it can be considered that the coating has failed and decision measures for repairing or repainting the coating are needed.

4.3. Corrosion Function Model of Epoxy Coating on Steel Bridges

According to the corrosion laws and mechanisms of coatings, the corrosion area rate and thickness of coatings exhibit nonlinear patterns with corrosion time. Research has shown that coating thickness and coating corrosion area rate can effectively characterize the degree of coating corrosion. Therefore, this paper takes coating thickness and coating corrosion area rate as model indicators to establish a nonlinear corrosion function model for epoxy coatings on steel bridges under accelerated corrosion environment. Dr. Yamamoto Takashi, a Japanese anti-corrosion expert, proposed the theory of coating corrosion life, which suggests that coating corrosion goes through two stages [35]. The first stage is corrosion before the coating is perforated, and the second stage is corrosion after the coating is perforated. This theory is consistent with the corrosion law obtained through experiments in this paper.

Based on the corrosion law of coatings and Dr. Yamamoto Takashi's coating life theory, this paper divides the corrosion process of epoxy coatings on steel bridges into two stages: the early stage of corrosion, the middle and later stage of corrosion. The early stage of corrosion refers to the period from the service of the coating to the occurrence of corrosion rust spots. During this stage, the corrosion of the coating is mainly characterized by a decrease in coating thickness. The middle and later stage of corrosion is from the appearance of corrosion rust spots to the failure of the coating. During this stage, the corrosion of the coating is mainly characterized by an increase in the corrosion area. Therefore, this paper divides the nonlinear corrosion function model of epoxy coating on steel bridges under accelerated corrosion environment into two parts. In the early stage of corrosion, the loss rate of coating thickness is used as the model indicator, and a function model for the early stage of epoxy coating corrosion on steel bridges under accelerated corrosion environment is established. In the middle and later stages of corrosion, the corrosion area rate of coating is used as the model indicator, and a function model for the middle and later stages of epoxy coating corrosion on steel bridges under accelerated corrosion environment is established.

The nonlinear corrosion function model of epoxy coatings on steel bridge in the early stage is shown in the Eq (3).

$$H = n + B_1 \times t + B_2 \times t^2 \quad (3)$$

Where, H : coating thickness loss rate, t : corrosion time (days), n : initial coating thickness loss rate (the initial coating thickness loss rate of the new coating is 0), B_1 and B_2 : constant (the values vary under different corrosive environments, as shown in Table 5).

Table 5. Parameter values of new coating under different corrosion environment

corrosion environment	n	B_1	B_2
	value	value	value
Freshwater environment	0	2.26E-4	1.43E-5
Saltwater environment	0	6.08E-4	1.01E-5

The nonlinear corrosion function model of epoxy coatings on steel bridge in the middle and later stages is shown in the Eq (4).

$$S = a \times b^t \quad (4)$$

Where, S : corrosion area rate, t : corrosion time (days), a and b : constant (the values vary under different corrosive environments, as shown in Table 6).

Table 6. Parameter values under different corrosion environment

corrosion environment	a	b
	value	value
Freshwater environment	2.98E-10	4.00
Saltwater environment	3.76E-08	2.96

5. Conclusions

This paper adopted the accelerated corrosion test method to study the corrosion law of epoxy coatings on steel bridges. An image processing algorithm based on MATLAB was performed grayscale conversion, normalized histogram drawing, and binary image processing on the surface morphology images of coated specimens. From the test results, the following conclusions could be drawn:

- Whether in freshwater or saltwater corrosion environment, the coatings on steel bridge will undergo varying degrees of corrosion, manifested by a decrease in coating thickness and an increase in corrosion area rate. The corrosion rate of the coating exhibits a non-linear corrosion pattern of slow corrosion in the early stage and accelerated corrosion in the middle and later stages.
- The experimental results indicate that the corrosion rate of epoxy coatings on steel bridges is faster in saltwater environment than in freshwater environment. Chlorine ions in salt environment can accelerate the corrosion of coatings. Chlorine ions are more likely to penetrate the coating and enter the coating/metal interface. Prolonged exposure to aqueous solutions can accelerate the corrosion reaction and easily penetrate the protective film on the metal surface, causing crevice corrosion and pitting corrosion.
- According to the analysis of coating morphology, it can be concluded that the surface of the coated specimens showed varying degrees of corrosion after the cyclic accelerated corrosion test for 90 days. The corrosion area rate of the coated specimens in a saline environment was higher. The image processing algorithms based on MATLAB can clearly present the corrosion morphology and degree of coating corrosion.

Based on the analysis of the mechanism of coating corrosion and the results of accelerated corrosion test, a nonlinear corrosion function model for steel bridge coatings in an accelerated corrosion environment was established. This function model has a high correlation with experimental data. Nonlinear corrosion function models were established for epoxy coatings in freshwater and saline environments, respectively.

Acknowledgement

This research did not receive any specific grant from funding agencies in the public, commercial, or not-for-profit sectors.

References

- [1] Abass AO. Recent advances on organic coating system technologies for corrosion protection of offshore metallic structures. *Journal of Molecular Liquids*, 2018, 269: 572-606. <http://doi.org/10.1016/j.molliq.2018.08.053>
- [2] Sørensen PA, Kiil S, et al. Anticorrosive coatings: a review. *J. Coat. Technol. Res.* 2009; 6: 135-176. <http://doi.org/10.1007/s11998-008-9144-2>

- [3] Meng F, Liu Y et al. Studies on Mathematical Models of Wet Adhesion and Lifetime Prediction of Organic Coating/Steel by Grey System Theory. *Materials*. 2017; 10: 1-15. <http://doi.org/10.3390/ma10070715>
- [4] Mansfeld F, Kenkel JV. Electrochemical Measurements of Time-of-Wetness and Atmospheric Corrosion Rates. *Corrosion*. 1977; 33: 13-16. <https://doi.org/10.5006/0010-9312-33.1.13>
- [5] Mansfeld F, Kendig MW, Tsai S. Evaluation of Corrosion Behavior of Coated Metals with AC Impedance Measurements. *Corrosion*. 1982; 38: 478-485. <https://doi.org/10.5006/1.3577363>
- [6] Salmasifar A, Sarabi AA, Mohammadloo HE. Anticorrosive performance of epoxy/clay nanocomposites pretreated by hexafluorozirconic acid based conversion coating on St 12. *Corros. Eng. Sci. Technol*. 2015; 50: 372-379. <http://doi.org/10.1179/1743278214Y.0000000233>
- [7] Lee CY, Lee SK, Park JH, et al. Novel approach to correlate degree of surface deterioration to coating impedance for laboratory test panels coated with two types of primers. *Corros. Eng. Sci. Technol*. 2012; 47: 411-420. <http://doi.org/10.1179/1743278212Y.000000015>
- [8] Kendig M, Scully J. Basic Aspects of Electrochemical Impedance Application for the Lifetime Prediction of Organic Coatings on Metals. *Corrosion*. 1990; 46: 22-29. <https://doi.org/10.5006/1.3585061>
- [9] Kirthiga, R., Elavenil, S. A survey on crack detection in concrete surface using image processing and machine learning. *J Build Rehabil*. 2024; 9:15. <http://doi.org/10.1007/S41024-023-00371-6>
- [10] Shengan Z, et al. Detection method of interface defects of titanium nitride thin film coating materials based on image processing. *International Journal of Materials and Product Technology* 65.1(2022):41-51. <http://doi.org/10.1504/IJMPT.2022.124256>
- [11] Sprague A, et al. Automatic Nondestructive Detection of Damages in Thermal Barrier Coatings Using Image Processing and Machine Learning. *Microscopy and Microanalysis* 28.S1(2022):3068-3072. <http://doi.org/10.1017/S1431927622011448>
- [12] Wenjun Y, et al. A novel method for evaluating the slurry coating characteristics of sized yarns based on the starch-iodine color reaction principle and image processing. *Textile Research Journal* 91.11-12(2021):1302-1312. <http://doi.org/10.1177/0040517520980805>
- [13] Perumal P, et al. Investigation of TiN coating uniformity and its corrosion behaviour using image process. *Materials Research Express* 6.4(2019):046411-046411. <http://doi.org/10.1088/2053-1591/aafae9>
- [14] Fernández-Isla C, Navarro J P, Alcover M P. Automated Visual Inspection of Ship Hull Surfaces Using the Wavelet Transform. *Mathematical Problems in Engineering*; 2013, 27(5): 211-244. <http://doi.org/10.1155/2013/101837>
- [15] Jahanshahi MR, Masri SF. Effect of color space, color channels, and sub-image block size on the performance of wavelet-based texture analysis algorithms: an application to corrosion detection on steel structures. *Computing in Civil Engineering*; 2013: 685-692. <https://doi.org/10.1061/9780784413029.086>
- [16] Son H, Hwang N, et al. Rapid and automated determination of rusted surface areas of a steel bridge for robotic maintenance systems. *Automation in Construction*; 2014, 42: 13-24. <http://doi.org/10.1016/j.autcon.2014.02.016>
- [17] Xie X. A review of recent advances in surface defect detection using texture analysis techniques. *ELCVIA: Electronic Letters on Computer Vision and Image Analysis*, 2008, 7(3): 1-22. <http://doi.org/10.5565/rev/elcvia.268>
- [18] Zaidan BB, Zaidan AA, Alanazi HO, et al. Towards corrosion detection system. *International Journal of Computer Science*, 2010, 7(3): 33-36.

- [19] Acosta MRG, Diaz JCV, Castro NS. An innovative image-processing model for rust detection using perlin noise to simulate oxide textures. *Corrosion Science*, 2014, 88: 141-151. <http://doi.org/10.1016/j.corsci.2014.07.027>
- [20] Chen PH, Shen HK, Lei CY, et al. Fourier-transform-based method for automated steel bridge coating defect recognition. *Procedia Engineering*, 2011, 14: 470-476. <https://doi.org/10.1016/j.proeng.2011.07.058>
- [21] Aijazi AK, Malaterre L, Tazir ML, et al. Detecting and analyzing corrosion spots on the hull of large marine vessels using colored 3d lidar point clouds. *ISPRS Annals of Photogrammetry Remote Sensing & Spatial Informa*, 2016, 33: 153-160.
- [22] Igoe D, Parisi AV. Characterization of the corrosion of iron using a smartphone camera. *Instrumentation Science and Technology*, 2016, 44(2): 139-147. <http://doi.org/10.1080/10739149.2015.1082484>
- [23] Kim I T, Itoh Y. Accelerated exposure tests as evaluation tool for estimating life of organic coatings on steel bridges. *Corros. Eng. Sci. Technol.* 2007; 42: 242-252. <http://doi.org/10.1179/174327807X214833>
- [24] Hirohata M, Takemi J, Itoh Y. Corrosion accelerated exposure experiment simulating under seawater environment for organic coated steel materials. *Corros. Eng. Sci. Technol.* 2014; 50: 449-461. <http://doi.org/10.1179/1743278214Y.0000000238>
- [25] Kallias, Alexandros N, et al. Performance profiles of metallic bridges subject to coating degradation and atmospheric corrosion. *Structure and Infrastructure Engineering*, 2017, 13(4):440-453. <http://doi.org/10.1080/15732479.2016.1164726>
- [26] Lee CY, Chang T. Service Life Prediction for Steel Bridge Coatings with Type of Coating Systems. *Korean Society of Steel Construction*. 2016; 28: 325-335. <http://doi.org/10.7781/kjoss.2016.28.5.325>
- [27] Fredj N, Cohendoz S, Feaugas X, et al. Ageing of marine coating in natural and artificial seawater under mechanical stresses. *Prog. Org. Coat.* 2012; 74: 391-399. <http://doi.org/10.1016/j.porgcoat.2011.10.002>
- [28] Fredj N, Cohendoz S, Feaugas X et al. Effect of mechanical stress on kinetics of degradation of marine coatings. *Prog. Org. Coat.* 2008; 63: 316-322. <http://doi.org/10.1016/j.porgcoat.2008.05.001>
- [29] Fredj N, Cohendoz S, Feaugas X, et al. Effect of mechanical stress on marine organic coating ageing approached by EIS measurements. *Prog. Org. Coat.* 2011; 72: 260-268. <http://doi.org/10.1016/j.porgcoat.2011.04.014>
- [30] Itoh Y, Kim IT. Accelerated cyclic corrosion testing of structural steels and its application to assess steel bridge coatings. *Anti-Corros. Methods Mater.* 2006; 53: 374-381. <http://doi.org/10.1108/00035590610711723>
- [31] Merachtsaki D, Xidas P, Giannakoudakis P, Triantafyllidis K, Spathis P. Corrosion Protection of Steel by Epoxy-Organoclay Nanocomposite Coatings. *Coatings*. 2017; 7(7):84. <https://doi.org/10.3390/coatings7070084>
- [32] Rachid H. Review on epoxy polymers and its composites as a potential anticorrosive coatings for carbon steel in 3.5% NaCl solution: Computational approaches. *Journal of Molecular Liquids*. 2021;336. <https://doi.org/10.1016/j.molliq.2021.116307>
- [33] ISO 8501-2007, "Preparation of steel substrates before application of paints and related products-Visual assessment of surface cleanliness-Part 1: Rust grades and preparation grades of uncoated steel substrates and of steel substrates after overall removal of previous coatings". Geneva, Switzerland: ISO 2007.
- [34] GB/T 1727-2021, "General methods for preparation of coating films". Beijing, China: GB/T 2021.(in Chinese)
- [35] Fang Z. Simple talk about the forecast theory about coating's life. *Paint Coat. Plat.* 2005; 3: 3-5. (in Chinese)